Isotope shift, nonlinearity of King plots, and the search for new particles

V. V. Flambaum,[1,2] A. J. Geddes,[1] and A. V. Viatkina[2]
[1]*School of Physics, University of New South Wales, Sydney 2052, Australia*
[2]*Helmholtz Institute Mainz, Johannes Gutenberg University, 55099 Mainz, Germany*

(Received 7 December 2017; published 19 March 2018)

We derive a mean-field relativistic formula for the isotope shift of an electronic energy level for arbitrary angular momentum; we then use it to predict the spectra of superheavy metastable neutron-rich isotopes belonging to the hypothetical island of stability. Our results may be applied to the search for superheavy atoms in astrophysical spectra using the known values of the transition frequencies for the neutron-deficient isotopes produced in the laboratory. An example of a relevant astrophysical system may be the spectra of the Przybylski's star where superheavy elements up to $Z = 99$ have been possibly identified. In addition, it has been recently suggested to use the measurements of King plot nonlinearity in a search for hypothetical new light bosons. On the other hand, one can find the nonlinear corrections to the King plot arising already in the standard model framework. We investigate contributions to the nonlinearity arising from relativistic effects in the isotope field shift, the nuclear polarizability, and many-body effects. It is found that the nuclear polarizability contribution can lead to the significant deviation of the King plot from linearity. Therefore, the measurements of the nonlinearity of King plots may be applied to obtain the nuclear polarizability change between individual isotopes. We then proceed with providing a rough analytical estimate of the nonlinearity arising solely from the effect of a hypothetical scalar boson. Our predictions give theoretical limitations on the sensitivity of the search for new interactions and should help to identify the most suitable atoms for corresponding experiments.

DOI: 10.1103/PhysRevA.97.032510

I. INTRODUCTION

Isotope shift (IS) phenomena in heavy atoms are an important way of probing various scenarios in nuclear physics and can aid the search for new physics beyond the standard model.

Nuclear theory predicts the existence of long-lived isotopes for elements with $Z \geqslant 104$ (see, e.g., Refs. [1,2]), in particular isotopes with a magic neutron number $N = 184$. However, producing these neutron-rich isotopes in laboratories by colliding lighter atoms is currently impossible. The Coulomb repulsion for nuclei grows as Z^2; in order to compensate for this with the attractive strong force, the neutron number N must grow more quickly than Z. Consequently, an isotope from the island of stability with $N = 184$ cannot be produced from the collision of a pair of lighter isotopes with smaller N/Z ratios.

In contrast to laboratories, various astrophysical events such as supernovae explosions, neutron star–black hole and neutron star mergers generate high neutron fluxes and may create environments favorable for the production of neutron-rich heavy elements. For example, a new mechanism of such a kind due to the capture of the neutron star material by a primordial black hole has been suggested in Ref. [3]. Furthermore, neutron star–neutron star mergers are predicted to generate optimal environments for the production of heavy atoms [4,5]. As a consequence, astrophysical data may be the best place to observe superheavy metastable elements. It is possible that optical lines of elements up to $Z = 99$ have already been identified in the spectra of Przybylski's star [6]. These elements include heavy, short-lived isotopes which may be products of the decay of long-lifetime nuclei near the island of stability [7].

IS calculations for superheavy elements can help trace the hypothetical island of stability in existing astrophysical data. It may be possible to predict a spectral line of a neutron-rich isotope ν' based on the experimental spectrum of a neutron-poor isotope ν and calculations of IS $\delta\nu$ as $\nu' = \nu + \delta\nu$. The results can then be used to search for the long-lifetime neutron-rich elements in complicated astrophysical spectra such as that of Przybylski's star.

Spectroscopic measurements of IS may also be relevant to the search for strange matter. Strange nuclei consist of up, down, and strange quarks (see Ref. [8] and references therein). A strange-matter nuclei of charge Z would have a very different radius in comparison to any regular isotope. A formula for IS can be used to predict the effects of this change in radius on atomic spectra.

Accurate numerical calculations of IS for heavy and superheavy elements are usually carried out using sophisticated many-body theory, for example, combining a configuration interaction (CI) and many-body perturbation theory approach (MBPT) (see, e.g., Refs. [7] and the references therein). However, in the absence of experimental data a simple analytical formula may be useful for quick estimates of IS and better qualitative understanding of this phenomenon. In the present work, we derive a relativistic mean-field analytic formula for the field shift, which is the dominating source of IS in heavy atoms. Since the relative magnitude of the many-body corrections to the mean-field case is approximately the same for atoms with similar electronic structure of outer shells, our formula may be used to make reasonable extrapolations from the experimental data of lighter atoms to superheavy elements where no data are available.

It should be noted that relativistic corrections produce an important difference in the dependence of the field shift on the nuclear radius r. The traditional expression for field shift is known as $F_i\delta\langle r^2\rangle$ where F_i is an electronic structure factor and $\delta\langle r^2\rangle$ is a nuclear parameter. Instead, the field shift in a relativistic approach should be written as $\tilde{F}_i\delta\langle r^{2\gamma}\rangle$ where $\gamma = \sqrt{(j+1/2)^2 - Z^2\alpha^2}$, j is the electron angular momentum, and α is the fine structure constant; the electronic factor $\tilde{F}_i$ is calculated in the present work. If one insists on using the traditional formula for the field shift $F_i\delta\langle r^2\rangle$, the factor F_i will depend on the nuclear radius; i.e., there will be no factorization of the electron and nuclear variables.

Because of the relativistic effects in heavy atoms, the field shift of the $p_{1/2}$ orbital is comparable to that of the $s_{1/2}$: The ratio is $\sim(1-\gamma)/(1+\gamma)$. The $Z\alpha$ expansion gives the ratio $\sim Z^2\alpha^2/4$ but for $Z = 137$, $\gamma \approx 0$, and for the superheavy elements the ratio tends to 1. For $j > 1/2$, the direct mean-field single-particle field shift is small. However, the mean-field rearrangement effect (the correction to the atomic potential δV due to the perturbation of the s and $p_{1/2}$ orbitals by the field-shift operator) produces the same dependence of field shift on nuclear radius for all orbitals: $\tilde{F}_i\delta\langle r^{2\gamma}\rangle$, where $\gamma = [1 - Z^2\alpha^2]^{1/2}$.

Our formula for the field shift allows us to estimate the King-plot nonlinearity of a given element. New long-range forces such as Yukawa-type interactions between electrons and nuclei can lead to nonlinearities in a King plot for a series of isotopes [9]. It is useful to understand other possible sources of nonlinearities in the IS in order to constrain new physics beyond the standard model. We estimate the mean-field rearrangement corrections and quadratic effects in the field shift. We also estimate the contribution to IS from the nuclear polarizability which is found to give a bigger contribution to the King-plot nonlinearity than the relativistic corrections to the field shift. This fact in principle allows an experimental probe of the change of nuclear polarizability between isotopes based on measuring the King plot nonlinearity, under the assumption that the effect of possible new physics interactions is negligible.

II. FIELD SHIFT IN THE MEAN FIELD APPROXIMATION

In Refs. [10,11], the Racah-Rosenthal-Breit formula for IS of s-wave energy levels was derived using first-order perturbation theory. However, it is found that for relativistic cases the formula is unjustified, as it relies on perturbation theory using the Coulomb wave functions for a pointlike nucleus when finding the correction to the energy due to the finite nuclear size. This is not valid because, while the energy perturbation due to the potential inside the nucleus is small, the perturbed and nonperturbed wave functions within this region are completely different. Indeed, the relativistic wave functions for $s_{1/2}$ and $p_{1/2}$ orbitals tend to infinity at $r = 0$ while for the finite nucleus they remain finite. This problem was already recognized by the authors of the initial publication and since then numerous attempts have been made to account for this large wave function distortion (see Ref. [12] and references therein). Furthermore, it should be pointed out that a high-precision analytical formula for the finite nuclear-size corrections in one-electron atoms and ions was developed, taking into account the fine details of nuclear charge distribution [13]. However, our goal is to obtain results for many-electron atoms and ions. In this work, we aim to find a simple analytical expression of the field shift in many-electron atoms for arbitrary valence electron angular momenta j,l based on the first-order perturbation theory, but starting from a more realistic initial approximation than a pointlike nucleus.

A. Mean-field isotope shift in many-electron atoms for arbitrary orbital angular momentum

The dominant contribution to IS in heavy atoms is the field shift arising from the change of nuclear radius, rather than the mass shift which is smaller [14]. Let us first consider a model allowing for the estimation of field shift for wave functions with arbitrary Dirac quantum numbers j and l, where $j = l \pm \frac{1}{2}$. Through this work, we assume the nucleus to be a uniformly charged sphere of radius R. The nuclear electric potential is

$$V(r,R) = \begin{cases} \frac{-Ze^2}{r} & \text{for } r \geqslant R\,, \\ \frac{-Ze^2}{R}\left(\frac{3}{2} - \frac{r^2}{2R^2}\right) & \text{for } r \leqslant R\,. \end{cases} \tag{1}$$

In superheavy nuclei, $V - \frac{Z}{r}$ (the difference between a finite-size and pointlike nucleus) is not a small perturbation (we remind the reader of the collapse of the spectrum for a pointlike nucleus with $Z = 137$). The perturbation used in this work is the change of the potential due to a small relative change of nuclear radii between isotopes, which can be defined as

$$\delta V = \frac{dV(r,R)}{dR}\delta R = \frac{3}{2}\frac{Ze^2}{R}\left(1 - \frac{r^2}{R^2}\right)\frac{\delta R}{R}. \tag{2}$$

Using perturbation theory and integrating over the nucleus, we can find the shift in energy as

$$\delta E_\kappa = \int_{\text{nuc.}} \Psi_\kappa^\dagger \delta V \Psi_\kappa d\vec{r}\,. \tag{3}$$

Radial parts of wave functions can be found from the following Dirac system of radial equations:

$$\begin{cases} (\frac{d}{dr} + \frac{\kappa}{r})rf(r) = (m + E - V)rg(r), \\ (\frac{d}{dr} + \frac{\kappa}{r})rg(r) = (m - E + V)rf(r), \end{cases} \tag{4}$$

where $\kappa = \mp(j + \frac{1}{2})$, and $f(r)$ and $g(r)$ are the upper and lower radial components of the Dirac spinor respectively. We approximate the potential energy near $r = 0$ to be constant:

$$u = V(0) = -\frac{3Ze^2}{2R}, \quad E,m \ll u. \tag{5}$$

After equating $F = rf(r)$ and $G = rg(r)$, we find that

$$\begin{cases} F' + \frac{\kappa}{r}F + uG = 0\,, \\ G' - \frac{\kappa}{r}G - uF = 0\,. \end{cases} \tag{6}$$

One can check that the solutions at small distances can be written as

$$\kappa < 0 \;:\; F = ar^{|\kappa|} + a_1 r^{|\kappa|+2}\,, \quad G = \frac{au}{2|\kappa|+1}r^{|\kappa|+1},$$

$$\kappa > 0 \;:\; G = br^{|\kappa|} + b_1 r^{|\kappa|+2}\,, \quad F = -\frac{bu}{2|\kappa|+1}r^{|\kappa|+1}.$$

where a, b are normalization constants and

$$a_1 = -\frac{u^2 a}{2(2|\kappa|+1)}\,, \quad b_1 = -\frac{u^2 b}{2(2|\kappa|+1)}.$$

Here we neglected higher orders in r^2/R^2; see also Ref. [15]. More accurate calculations have demonstrated that their contribution to the field shift is small (see next subsection).

It can be shown that in both cases

$$(F^2+G^2) \propto r^{2|\kappa|}\left[1-\frac{9}{2}\frac{Z^2\alpha^2|\kappa|}{(2|\kappa|+1)^2}\left(\frac{r}{R}\right)^2\right]. \tag{7}$$

To determine the field shift, we match the expression for the radial density f^2+g^2 inside the nucleus to the radial density outside the nucleus. At the surface, $\rho_{\rm inside} = \rho_{\rm outside}$, since ρ is continuous. Near the nucleus, the nuclear Coulomb potential is not screened, and all atomic wave functions are proportional to the corresponding Coulomb wave functions. Therefore, we use expressions of these wave functions at small distances (presented in Appendix C) to approximate the radial density at the nuclear surface ($r = R$):

$$\begin{aligned}\rho_{\rm surface} &= f^2_{\rm surface} + g^2_{\rm surface} \\ &= \frac{1}{(z_i+1)}\frac{Z}{a_B^3}\left(\frac{I}{\rm Ry}\right)^{3/2}\frac{4}{[\Gamma(2\gamma+1)]^2}\left(\frac{a_B}{2ZR}\right)^{2-2\gamma} \\ &\quad\times 2\kappa(\kappa-\gamma)\,,\end{aligned} \tag{8}$$

where $\gamma = \sqrt{\kappa^2 - Z^2\alpha^2}$, $I = \frac{(z_i+1)^2}{\nu^2}{\rm Ry}$ is the ionization energy for an orbital with effective principal quantum number ν in the ion of charge z_i, and ${\rm Ry} = \frac{e^2}{2a_B}$ is the Rydberg constant. As shown above, the electron density inside the nucleus behaves approximately as

$$\rho(r) \approx \rho_{\rm surface}\left(\frac{r}{R}\right)^{2(|\kappa|-1)}. \tag{9}$$

This expression approximates the electron density inside the nucleus significantly better than the Coulomb solution and should give more accurate results than the Racah-Rosenthal-Breit approach. Corrections to Eqs. (7)–(9) are in the next subsection. Their contribution to the isotope shift is small.

Using Eq. (3) and introducing $x = r/R$, one can find that

$$\begin{aligned}\delta E_\kappa &= \frac{3}{2}Ze^2R^2\frac{\delta R}{R}\int_0^1 \left(f_\kappa^2+g_\kappa^2\right)(1-x^2)x^2dx \\ &= \frac{3}{2}Ze^2R^2\frac{\delta R}{R}\int_0^1 \rho_{sf}x^{2(|\kappa|-1)}(1-x^2)x^2dx,\end{aligned} \tag{10}$$

which gives

$$\begin{aligned}\delta E_\kappa &= \frac{1}{(z_i+1)}\frac{12\kappa(\kappa-\gamma)}{(2|\kappa|+1)(2|\kappa|+3)[\Gamma(2\gamma+1)]^2} \\ &\quad\times\left(\frac{2ZR}{a_B}\right)^{2\gamma}\frac{I^{3/2}}{{\rm Ry}^{1/2}}\frac{\delta R}{R}\,.\end{aligned} \tag{11}$$

B. Isotope shift for s and $p_{1/2}$ waves

From Eq. (7), we see that $Z^2\alpha^2r^2/R^2$ corrections to the electron density decrease with the increase of $|\kappa|$. Indeed, the ratio of the potential $|V|$ and the centrifugal term $|\kappa|/r$ in the Dirac equation decreases as $1/|\kappa|$. Therefore, to analyze the role of the corrections it is sufficient to consider the case of the minimal $|\kappa| = 1$, of s ($\kappa = -1$) and $p_{1/2}$ ($\kappa = 1$) waves. These are also the most important cases for the isotope shift.

The potential inside the nucleus $V = \frac{-Ze^2}{R}(\frac{3}{2} - \frac{r^2}{2R^2})$ is quadratic and wave functions inside the nucleus correspond to the solutions for the relativistic oscillator. These solutions must be matched with the Coulomb solutions outside the nucleus.[1] The result may be presented in the following form (see, e.g., Ref. [16]):

$$\Psi_{s_{1/2}} = \begin{pmatrix} f_s\Omega_s \\ ig_s\Omega_{p_{1/2}}\end{pmatrix}, \tag{12}$$

$$\Psi_{p_{1/2}} = \begin{pmatrix} -\frac{A_p}{A_s}\,g_s\Omega_{p_{1/2}} \\ i\frac{A_p}{A_s}\,f_s\Omega_s\end{pmatrix}, \tag{13}$$

where f_s, g_s, A_s, and A_p are defined in Appendix A. As before, we treat the change in the potential within the nucleus due to the isotope effect (2) as our perturbation. Again, we find the energy shifts:

$$\delta E_s = \frac{3}{2}Ze^2R^2\frac{\delta R}{R}\int_0^1 \left(f_s^2+g_s^2\right)(1-x^2)x^2dx\,, \tag{14}$$

$$\begin{aligned}\delta E_{p_{1/2}} &= \frac{3}{2}Ze^2R^2\left(\frac{A_p}{A_s}\right)^2\frac{\delta R}{R} \\ &\quad\times\int_0^1 \left(g_s^2+f_s^2\right)(1-x^2)x^2dx\,.\end{aligned} \tag{15}$$

These expressions for the isotope shift are evaluated and expanded over small $Z^2\alpha^2$ to give

$$\begin{aligned}\delta E_s &= \frac{1}{z_i+1}\frac{1}{[\Gamma(2\gamma+1)]^2}\left(\frac{2ZR}{a_B}\right)^{2\gamma}\frac{I_s^{3/2}}{{\rm Ry}^{1/2}} \\ &\quad\times\frac{4}{5}(1-0.24Z^2\alpha^2)\frac{\delta R}{R}\,,\end{aligned} \tag{16}$$

$$\begin{aligned}\delta E_p &= \frac{1}{z_i+1}\frac{Z^2\alpha^2}{[\Gamma(2\gamma+1)]^2}\left(\frac{2ZR}{a_B}\right)^{2\gamma}\frac{I_p^{3/2}}{{\rm Ry}^{1/2}} \\ &\quad\times\frac{1}{5}(1+0.26Z^2\alpha^2)\frac{\delta R}{R}\,.\end{aligned} \tag{17}$$

Up to corrections $\pm 0.01Z^2\alpha^2$, these two expressions may be presented as one equation:

$$\begin{aligned}\delta E_{|\kappa|=1} &= \frac{4}{5}\frac{1}{z_i+1}\frac{\kappa(\kappa-\gamma)}{[\Gamma(2\gamma+1)]^2} \\ &\quad\times\left(\frac{2ZR}{a_B}\right)^{2\gamma}\frac{I^{3/2}}{{\rm Ry}^{1/2}}\frac{\delta R}{R}.\end{aligned} \tag{18}$$

One can see that the expression (18) directly follows from (11), if we put $|\kappa| = 1$. Estimates show that the higher order correction $\sim Z^4\alpha^4$ comes with a small coefficient.

[1] These Coulomb solutions include regular and irregular at $r = 0$ components.

TABLE I. Estimates of the isotope shift $\delta\nu$ [using Eq. (11)] for a given transition in superheavy atoms. A_1 is the atomic number of already synthesized reference isotope. $A_2 = Z + 184$ is the isotope of a given element belonging to the hypothetical island of stability with magic neutron number $N = 184$.

Atom Symbol	Z	A_1	A_2	Transition	$\delta\nu$ (cm^{-1})	$\delta\nu$ (GHz)
Cf	98	251	282	$5f^{10}7s^2 \to 5f^{10}7s7p$	−7.3	−218
Es	99	252	283	$5f^{11}7s^2 \to 5f^{11}7s7p$	−7.8	−233
Fm	100	257	284	$5f^{12}7s^2 \to 5f^{12}7s7p$	−7.7	−230
Md	101	258	285	$5f^{13}7s^2 \to 5f^{13}7s7p$	−8.5	−255
No	102	259	286	$7s^2 \to 7s7p$	−9.6	−286
Lr	103	266	287	$7s^27p \to 7s^28s$	0.78	23.3
Rf	104	263	288	$6d^27s^2 \to 6d^27s7p$	−11.5	−344
Db	105	268	289	$6d^37s^2 \to 6d^37s7p$	−11.7	−351
Sg	106	269	290	$6d^47s^2 \to 6d^47s7p$	−14.1	−424
Bh	107	270	291	$6d^57s^2 \to 6d^57s7p$	−17.1	−511
Hs	108	269	292	$6d^67s^2 \to 6d^67s7p$	−22.3	−670
Mt	109	278	293	$6d^77s^2 \to 6d^77s7p$	−17.3	−518
Ds	110	281	294	$6d^87s^2 \to 6d^87s7p$	−17.8	−533
Rg	111	282	295	$6d^97s^2 \to 6d^97s7p$	−21.1	−632
Cn	112	285	296	$6d^{10}7s^2 \to 6d^{10}7s7p$	−21.1	−633
Nh	113	286	297	$7s^27p \to 7s^28s$	−0.35	−10.5
Fl	114	292	298	$7p^2 \to 7p8s$	−0.64	−19.3

Note that the ratio of the isotope shifts for $p_{1/2}$ and $s_{1/2}$ is equal to

$$\left(\frac{A_p}{A_s}\right)^2 = \left(\frac{I_p}{I_s}\right)^{3/2} \frac{z^2\alpha^2}{4}\left(1+\frac{z^2\alpha^2}{4}\right)^2 \approx \left(\frac{I_p}{I_s}\right)^{3/2} \frac{1-\gamma}{1+\gamma}.$$

III. QUANTITATIVE FIELD SHIFT ESTIMATES

A. Estimates for field shifts in superheavy atoms

Table I depicts the estimates for isotope shift in superheavy atoms which were calculated using Eq. (18). The ionization potentials used to calculate the field shift for each level in a given atom has been detailed in Appendix D. Furthermore, the nuclear radius R was found using $R = r_0 A^{1/3}$, where we assumed that $r_0 = 1.15$ fm for the purpose of these calculations.

One of the motivations for the current work was to provide a simple method to estimate IS which is suitable for superheavy atoms and provides a better understanding of its dependence on the nuclear and atomic parameters. Accurate many-body calculations of the field shift for No, Lr, Nh, Fl, and Ra have recently been performed and presented in Ref. [7]. The CI+MBPT isotopic shift value for No was found to be $-7.28\,\mathrm{cm}^{-1}$. Our approximate IS value for No is $-9.6\,\mathrm{cm}^{-1}$ as presented in Table I. The difference is actually comparable to 20% error of the CI+MBPT value.

The calculated IS for Lr, Nh, and Fl is small due to large cancellations in the shifts between the lower p state and excited s state. We hence can provide only an order of magnitude estimates when calculating IS for transitions for $p \to s$ states using the method presented in this paper. Indeed, the $7p_{1/2}$ state IS is suppressed by the factor $(1-\gamma)/(1+\gamma)$ but enhanced by the higher $7p_{1/2}$ ionization potential than that of $8s$. This is why IS of $7p_{1/2}$ and $8s$ states nearly cancel each other out. While the absolute accuracy of IS calculations is the same, the relative accuracy of IS of the transition energy is poor. The value for the overall IS of Nh in our case is $-0.35\,\mathrm{cm}^{-1}$, which is significantly smaller than and opposite in sign to the CI+MBPT value for Nh, which was stated to be $1.42\,\mathrm{cm}^{-1}$. Similarly, we calculated an IS of $-0.64\,\mathrm{cm}^{-1}$ for Fl, which is the same order of magnitude as CI+MBPT value given as $0.12\,\mathrm{cm}^{-1}$ yet also opposite in sign. Our approximate value of IS for Lr is $0.78\,\mathrm{cm}^{-1}$, which is notably smaller then the CI+MBPT value of $3.134\,\mathrm{cm}^{-1}$. We reiterate that the relative accuracies of the analytical formula and the CI+MBPT method in these cases are low, and all that we can conclude is that the IS is small and the frequencies of the transitions in all isotopes will be approximately the same.

TABLE II. Comparison of experimental field shifts in Ca, Yb, and Hg with theoretical prediction based on formula (11) and experimental values of mean nuclear charge radii. Both measured field shifts and nuclear charge radii are found in Ref. [18].

Atom	A_1	A_2	Transition	$\delta\nu_{\mathrm{exper}}$ (MHz)	$\delta\nu_{\mathrm{theor}}$ (MHz)
Ca	46	48	$3p^64s^2 \to 3p^64s4p$	−25.3 ± 1.0	−31
Yb	174	176	$4f^{14}6s^2 \to 4f^{14}6s6p$	993 ± 250	1217
Hg	202	204	$5d^{10}6s^2 \to 6d^{10}6s6p$	5238 ± 11	4939

B. Estimates for field shifts in Ca, Ca^+, Yb, and Hg

We calculated field shifts of $s \to p$ transitions for Ca, Ca^+, Yb, and Hg to compare with known experimental data. The results are presented in Tables II and III. The agreement for s-p transitions is good. However, in the case of Ca^+, formula (11) underestimates the measured field shifts of $3p^63d\ ^2D_{3/2} \to 3p^64p\ ^2P_{1/2}$ transition [17] by two orders of magnitude. The reason is that the direct field IS in d-p transitions in light atoms is very small and the actual field IS is dominated by the mean-field rearrangement effect (the change of atomic potential due to the isotope shift in s and $p_{1/2}$ wave functions), which will be discussed in the next section.

IV. NON-LINEARITIES IN KING PLOT FOR ISOTOPE SHIFTS

As we will show below, the nonlinear corrections to the King plot may be due to the nonfactorization of the electronic and nuclear parameters in the expression for the field IS. This nonfactorization appears if we have two or more nuclear

TABLE III. Comparison of experimental field shifts for the $3p^64s\ ^2S_{1/2} \to 3p^64p\ ^2P_{1/2}$ transition in Ca^+ [17] with theoretical results using formula (11) and nuclear charge radii data from Refs. [18,19].

	MHz		
	$\delta\nu_{\mathrm{field}}^{40,42}$	$\delta\nu_{\mathrm{field}}^{40,44}$	$\delta\nu_{\mathrm{field}}^{40,48}$
Theory	−60.1	−85.2	−0.30
Exp.	−60.9(2.0)	−79.6(2.7)	1.27(1.69)

parameters which are not proportional to each other and appear in different combinations for different atomic transitions. As a rule, the second nuclear parameter gives a contribution to IS which is several orders of magnitude smaller than the contribution of the first nuclear parameter. This means that the nonlinearity is small.

A. King plot in the mean-field approximation

With $\mu_{AA'} = \frac{1}{m_A} - \frac{1}{m_{A'}}$, where the masses of isotopes A and A' are denoted as m_A and $m_{A'}$ respectively, the IS can be written as follows:

$$\nu_i^{AA'} = K_i \mu_{AA'} + F_i \delta\langle r^{2\gamma_1}\rangle_{AA'} + G_i \delta\langle r^{2\gamma_2}\rangle_{AA'}. \quad (19)$$

The first term expresses the mass shift, both normal and specific. The second term is the leading-order contribution to the field shift discussed in the previous section. For s-wave in the nonrelativistic limit ($\gamma_1 \to 1$), this term scales with the difference of mean squares of nuclear charge radii between the isotopes A and A': $\delta\langle r^2\rangle_{AA'}$. The third term expresses a correction to the field shift produced by higher waves. For example, for $p_{3/2}$ in the nonrelativistic limit, $\gamma_2 \to 2$ and $\delta\langle r^{2\gamma_2}\rangle_{AA'} = \delta\langle r^4\rangle_{AA'}$. A similar term may appear as a subleading correction to the s-wave field shift but it does not produce a contribution to the nonlinearity of the King plot since it only redefines the the main s-wave contribution $F_i\delta\langle r^{2\gamma_1}\rangle_{AA'}$; i.e., it produces a correction which is the same in different atomic transitions. The nonlinearity appears when the ratio G_i/F_i changes, as will be shown below.

Next we divide Eq. (19) by $\mu_{AA'}$ and hence define a new modified frequency $n_i = \nu_i^{AA'}/\mu_{AA'}$:

$$n_i = K_i + F_i x + G_i y\,, \quad (20)$$

with $x = \delta\langle r^{2\gamma_1}\rangle_{AA'}/\mu_{AA'}$ and $y = \delta\langle r^{2\gamma_2}\rangle_{AA'}/\mu_{AA'}$. Here $i = 1,2$ are the two transitions examined in a chain of isotopes. A plot of n_1 vs n_2 gives what is known as the King plot [20]. If we assume $G_{1,2} = 0$, one can write n_2 as a linear function of n_1; i.e., the King plot is linear. To trace the possible nonlinearity, we must consider at least four isotopes (A, A_1, A_2, A_3) forming three pairs, giving three points on the plot:

$$AA_1 \equiv a, \quad AA_2 \equiv b, \quad AA_3 \equiv c\,. \quad (21)$$

The first two points can be used to determine the gradient $k = (n_2^b - n_2^a)/(n_1^b - n_1^a)$. Let us state a hypothetical $\tilde{c}$ point, lying on the same line as a and b:

$$n_2^{\tilde{c}} = n_2^b + k\left(n_1^c - n_1^b\right). \quad (22)$$

Then the nonlinearity is defined (see Fig. 1) as

$$\mathrm{NL} \equiv \left(n_2^c - n_2^{\tilde{c}}\right)\mu_c\,, \quad (23)$$

where $\mu_c = \mu_{AA_3}$, and the value (23) can be expressed in hertz. Let us explicitly expand the difference between two modified frequencies:

$$n_2^c - n_2^{\tilde{c}} = K_2 + F_2 x^c + G_2 y^c - K_2 - F_2 x^b - G_2 y^b - \frac{F_2(x_b - x_a) + G_2(y_b - y_a)}{F_1(x_b - x_a) + G_1(y_b - y_a)}[F_1(x_c - x_b) + G_1(y_c - y_b)].$$

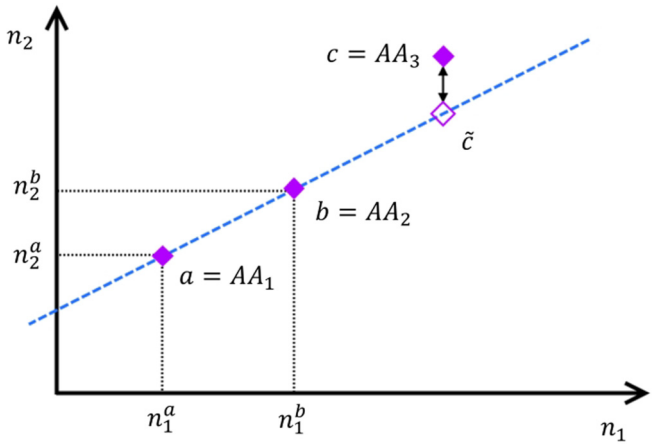

FIG. 1. Schematic illustration of the King plot nonlinearity. Modified frequencies n_1 and n_2 are plotted for the three pairs of isotopes (21). The difference between point c and the hypothetical point $\tilde{c}$ lying on the same line as a and b leads to the evaluation of nonlinearity of the plot (23).

Under the assumption of $\frac{G\Delta y}{F\Delta x} \ll 1$ and with $q_{ba} \equiv \frac{y_b - y_a}{x_b - x_a}$, one can show that

$$n_2^c - \tilde{n}_2^c = (x_c - x_b)(q_{cb} - q_{ba})\left(\frac{G_2}{F_2} - \frac{G_1}{F_1}\right)F_2. \quad (24)$$

Here we see that the nonlinear correction vanishes in two cases:

(1) $q_{cb} = q_{ba}$,

(2) $\frac{G_2}{F_2} = \frac{G_1}{F_1}$.

The first case considers $\delta\langle r^{2\gamma_1}\rangle$ and $\delta\langle r^{2\gamma_2}\rangle$. These parameters are correlated: Generally speaking, increase of the nuclear radius R leads to the increase of both $\delta\langle r^{2\gamma_1}\rangle$ and $\delta\langle r^{2\gamma_2}\rangle$. It is easy to check that if the field shift for all isotopes is completely defined by the change of the nuclear radius δR from isotope to isotope, i.e., if $\delta\langle r^{2\gamma}\rangle = D_\gamma \delta R$ for any δR (as in the linear approximation in δR), we have $q_{cb} = q_{ba}$.

For example, in the isotope shift (11) the dependence on R is given by $R^{2\gamma-1}\delta R$ and the difference between two isotopes is proportional to $R_A^{2\gamma-1}\delta R_{A\tilde{A}}$. This, given fixed reference isotope A, leads to $q_{cb} = q_{ba}$. Therefore, to get a nonzero result we should go beyond the first order in $\delta R/R$. We integrate formula (11) to effectively include all orders of perturbation theory in $\delta R/R$. Then the field shift of an energy level between isotopes A and $\tilde{A}$ is

$$\Delta E_\kappa = \frac{12\kappa(\kappa - \gamma)}{2\gamma(z_i + 1)(2|\kappa| + 1)(2|\kappa| + 3)[\Gamma(2\gamma + 1)]^2} \times \left(\frac{2Z}{a_B}\right)^{2\gamma} \frac{I^{3/2}}{\mathrm{Ry}^{1/2}}\left(R_{\tilde{A}}^{2\gamma} - R_A^{2\gamma}\right). \quad (25)$$

We plot the field shifts of transition frequencies $(\Delta E_{\kappa,\mathrm{upper}} - \Delta E_{\kappa,\mathrm{lower}})_{A\tilde{A}}$ for three pairs of isotopes of five elements: Ca^+, Sr^+, Ba^+, Yb^+, and Hg^+. Fitting a line to the first two pairs a and b, we find the nonlinearity as $(n_2^c - \tilde{n}_2^c)\mu_c$.

The results are presented in Table IV. In order to find the radii R for substituting into (25), we first make use of the simple liquid-drop model where $R = r_0 A^{\frac{1}{3}}$ (method 1 in Table IV). Then to obtain more realistic estimate, we find the equivalent

TABLE IV. Estimates for the nonlinearities of King plot [defined in Eq. (23)]. Methods 1 and 2 are based on the mean-field analytic expression of field isotope shift (25) found from the estimate of wave function density (9) in an uniformly charged spherical nucleus. Method 1 utilizes the liquid-drop approximation for nuclear radius $R = r_0 A^{\frac{1}{3}}$ with $r_0 = 1.15$ fm and method 2 uses experimental data [18,19] for mean squares of nuclear charge radii $\langle r^2 \rangle$ when finding the equivalent nuclear radius: $\langle r^2 \rangle = \frac{3}{5} R^2$. Method 3 accounts for both expression (25) and the contribution of nuclear polarizability (26), and equivalent nuclear radius R is again based on the experimental data; i.e., it is the most complete calculation in this table. We have not calculated these corrections and the nuclear polarizability contribution in s-p/d-p transitions in Ca^+ since they are expected to be similar to s-d transitions.

Ion	Z	A	A_1	A_2	A_3	Pair of transitions	Nonlinearity (Hz) Method 1	Method 2	Method 3
Ca^+	20	40	42	44	48	$3p^6 4s\ ^2S_{1/2} \to 3p^6 4p\ ^2P_{1/2}$ $3p^6 3d\ ^2D_{3/2} \to 3p^6 4p\ ^2P_{1/2}$	-1.2×10^{-4}	3.0×10^{-4}	
						$3p^6 4s\ ^2S_{1/2} \to 3p^6 3d\ ^2D_{3/2}$ $3p^6 4s\ ^2S_{1/2} \to 3p^6 3d\ ^2D_{5/2}$	-1.2×10^{-4}	3.0×10^{-4}	-6.6×10^{-2}
Sr^+	38	84	86	88	90	$4p^6 5s\ ^2S_{1/2} \to 4p^6 4d\ ^2D_{3/2}$ $4p^6 5s\ ^2S_{1/2} \to 4p^6 4d\ ^2D_{5/2}$	-1.1×10^{-3}	1.1×10^{-2}	-2.6
Ba^+	56	132	134	136	138	$5p^6 6s^1\ ^2S_{1/2} \to 5p^6 5d\ ^2D_{3/2}$ $5p^6 6s^1\ ^2S_{1/2} \to 5p^6 5d\ ^2D_{5/2}$	-3.6×10^{-3}	-3.9×10^{-2}	7.6
Yb^+	70	168	170	172	176	$4f^{14} 6s\ ^2S_{1/2} \to 4f^{13} 6s^2\ ^2F^o_{7/2}$ $4f^{14} 6s\ ^2S_{1/2} \to 4f^{14} 5d\ ^2D_{3/2}$	6.1×10^{-2}	-3.1	38
						$4f^{14} 6s\ ^2S_{1/2} \to 4f^{14} 5d\ ^2D_{3/2}$ $4f^{14} 6s\ ^2S_{1/2} \to 4f^{14} 5d\ ^2D_{5/2}$	-6.1×10^{-2}	3.1	-18
Hg^+	80	196	198	200	204	$5d^{10} 6s\ ^2S_{1/2} \to 5d^9 6s^2\ ^2D_{3/2}$ $5d^{10} 6s\ ^2S_{1/2} \to 5d^9 6s^2\ ^2D_{5/2}$	5.5×10^{-1}	3.1	-14

R from the experimental values of mean square nuclear charge radius [18,19] (method 2 in Table IV): $R^2 = \frac{5}{3}\langle r^2 \rangle$.

The expression (25) is, in fact, only the first-order contribution to the field shift in terms of energy. The second order in the single-electron mean-field approximation can be roughly estimated as a quadratic term $\pm(\Delta E_\kappa)^2/I$. Because of its smallness in higher waves ($\kappa \neq -1$) it has only a negligible effect on the King plot nonlinearity. But, as will be shown in Sec. IV C, if we include many-body corrections, this quadratic term can alter considerably the nonlinearity value in heavy atoms (the field shift is $\propto Z^{2\gamma}$, correspondingly the quadratic term should be $\propto Z^{4\gamma}$).

B. Nuclear polarizability effect

The nuclear structure effects for simple atoms have been considered in Ref. [21]. We are interested in such effects in many-electron atoms. The nuclear polarization potential produced by the nuclear polarizability α_p is a long-range one ($V_\alpha = -\frac{1}{2}\frac{\alpha_p e^2}{r^4}$, α_p having dimension $[l^3]$); therefore, it can give a significant contribution to a higher-wave isotope shift and overall nonlinearity of King plot. The main contribution to the corresponding energy shift comes from the area near the nucleus where the nuclear potential is not screened. In order to estimate the shift, we integrate the radial density $\rho_\kappa = f_\kappa^2 + g_\kappa^2$ using atomic wave functions proportional to the Coulomb wave functions outside the nucleus (see Appendix B) with the interaction Hamiltonian V_α:

$$\delta E_\alpha = \int_{r_0}^{+\infty} \left[f_\kappa^2(r) + g_\kappa^2(r)\right]\left(-\frac{1}{2}\frac{\alpha_p e^2}{r^4}\right) r^2 dr\ ,$$
$$r_0 = \begin{cases} R, & |\kappa| = 1\ , \\ 0, & |\kappa| > 1\ . \end{cases} \tag{26}$$

For $|\kappa| > 1$, the integral with the Coulomb wave functions converges at $r = 0$ and we may calculate it taking the cutoff parameter $r_0 = 0$. In this case, the general analytic solution can be presented here as

$$\delta E_\alpha = -\alpha_p \frac{9 + 5\kappa(\kappa - 3) + 5Z^2\alpha^2 + \gamma^2}{256\gamma[-9 + \gamma^2(7 - 4\gamma^2)^2]} \times \frac{8^3 Z^2}{a_B^3}\frac{2}{z_i + 1}\frac{I^{3/2}}{\mathrm{Ry}^{1/2}}\ , \tag{27}$$

where $\gamma = \sqrt{\kappa^2 - Z^2\alpha^2}$ and I is the ionization potential of the electron, a_B is the Bohr radius, Ry is the Rydberg constant, and z_i is the ion charge. For $|\kappa| = 1$, the integral in Eq. (26) from 0 would diverge, but a cutoff from the nuclear radius R would give a reasonable upper estimate of the effect.[2] Note that the s orbital always appears in both transitions which we compare in the King plot, and therefore the exact magnitude of this $|\kappa| = 1$ term is not important for the estimate of the nonlinearity.

To obtain the numerical values for the integral with $|\kappa| = 1$, we have used the Bessel function solutions from Appendix B; however, without loss of the actual numerical accuracy its adequate approximation can be found by substituting expressions for wave functions expanded at $r \to 0$ (see Appendix C) to the

[2]Actually, the polarization potential V_α becomes a nonlocal integration operator [22] starting from larger distances, $r < r_0 \sim 10$ fm, where the relativistic kinetic energy of electron $\sim \hbar c/r_0$ approaches $E \approx 20$ MeV. Here E is the excitation energy of the nuclear giant dipole resonance which gives the dominating contribution to the polarizability. This problem will be discussed in a future publication.

integral (26):

$$\delta E_\alpha = -\alpha_p \frac{8\kappa(\kappa-\gamma)}{3-2\gamma}\frac{1}{z_i+1}\frac{Z}{a_B^2} \times \frac{1}{[\Gamma(2\gamma+1)]^2}\left(\frac{a_B}{2Z}\right)^{2-2\gamma}\frac{I^{3/2}}{\mathrm{Ry}^{1/2}}R^{2\gamma-3}. \quad (28)$$

Although the ceiling estimate presented in Eq. (27) is utilized in subsequent calculations and is sufficient for the purpose of this work, an expression can be written specifically for the $s_{1/2}$ contributions to nuclear polarizability. The nonrelativistic expression for the energy shift has been derived in Ref. [23]:

$$\delta E_{\alpha,s} = -m_e c^2 \alpha \Psi(0)^2 \alpha_p \left[\frac{19}{6} + 5\ln\left(\frac{\bar{E}}{m_e c^2}\right)\right], \quad (29)$$

where $\bar{E}$ is the average nuclear excitation energy. Using the the nuclear oscillator model, we can estimate the excitation energy as the distance between the nuclear shells $\bar{E} = 40\ \mathrm{MeV}/A^{1/3}$. $\Psi(0)^2$ is the single valence electron density at the nucleus which, in the nonrelativistic limit, has the form of

$$\Psi(0)^2 = \frac{Z\left(\frac{I}{\mathrm{Ry}}\right)^{3/2}}{\pi a_B^3(z_i+1)}. \quad (30)$$

The expression for $\delta E_{\alpha,s}$ can be modified to include a relativistic factor that reflects the increase in the relativistic wave function toward the nucleus. To make a rough estimate of this factor, we chose the cutoff radius to be the Compton wavelength of an electron $k_e = \frac{\hbar}{m_e c}$ where the nonrelativistic approach breaks down:

$$R_{\mathrm{rel}} = \left(\frac{2Zk_e}{a_B}\right)^{2\gamma-2} \approx \left(\frac{1}{Z\alpha}\right)^{2(1-\gamma)}. \quad (31)$$

Incorporating R_{rel} with the nonrelativistic expression for $\delta E_{\alpha,s}$ we can present the expression

$$\delta E_{\alpha,s} = -m_e c^2 \alpha \frac{Z}{\pi a_b^3(z_i+1)}\left(\frac{I}{\mathrm{Ry}}\right)^{3/2}\alpha_p \quad (32)$$

$$\left[\frac{19}{6} + 5\ln\left(\frac{\bar{E}}{m_e c^2}\right)\right]R_{\mathrm{rel}}. \quad (33)$$

The relativistic factor can be written as $R_{\mathrm{rel}} \approx (Z\alpha)^{-Z^2\alpha^2}$ by expanding γ through by small $Z\alpha$. It follows that $R_{\mathrm{rel}} \approx e^{\ln((Z\alpha)^{-Z^2\alpha^2})}$ can be approximated as $R_{\mathrm{rel}} \approx 1 + Z^2\alpha^2\ln(\frac{1}{Z\alpha})$. Hence, it is apparent that the relativistic formulation of the $s_{1/2}$ contribution to nuclear polarizability differs from Eqs. (29) and (30) by less then a factor of 2.

An expression for nuclear polarizability α_E based on the giant resonance approach was obtained by Migdal [24,25]:

$$\alpha_p = \frac{e^2 R^2 A}{40\, a_{\mathrm{sym}}}. \quad (34)$$

We use the empirical value of the nuclear symmetry energy $a_{\mathrm{sym}} = 23$ MeV [26,27].

To the first order, one can treat the change of α_E as consisting of two independent parts, one resulting from the growth of nuclear radius ΔR and another from the change of nucleon number ΔA:

$$\Delta\alpha_p = \frac{2e^2 R}{40\, a_{\mathrm{sym}}} A\Delta R + \frac{e^2 R^2}{40\, a_{\mathrm{sym}}}\Delta A. \quad (35)$$

The second contribution can be independently evaluated using the nuclear oscillator model. From the second-order perturbation theory follows that with the addition of one neutron, the nuclear polarizability changes as

$$\delta\alpha_{p,\mathrm{A}+1} = -q_n^2\left[\frac{\langle n|x|n+1\rangle^2}{E_n - E_{n+1}} + \frac{\langle n|x|n-1\rangle^2}{E_n - E_{n-1}}\right]. \quad (36)$$

Here, $q_n = eZ/A$ is the effective charge of a neutron, originating from the recoil effect.[3] Energy levels of a quantum oscillator are known to be $E_n = \hbar\omega(n+\frac{1}{2})$ and its matrix elements can be written [28] as

$$\langle n|x|n+1\rangle^2 = \frac{(n+1)\hbar}{2M\omega}, \quad \langle n|x|n-1\rangle^2 = \frac{n\hbar}{2M\omega},$$

with the frequency ω for the case of nuclei and M being the neutron mass. Assuming $r_0 = 1.15$ fm, one can write

$$\omega = \frac{40\ \mathrm{MeV}}{\hbar}\frac{r_0}{R},$$

$$\Delta\alpha_{p,A} = \delta\alpha_{p,\mathrm{A}+1}\Delta A = \frac{e^2}{2M\omega^2}\left(\frac{Z}{A}\right)^2\Delta A = \frac{e^2\hbar^2}{2M}\left(\frac{Z}{A}\right)^2\left[\frac{R}{r_0 \times (40\ \mathrm{MeV})}\right]^2\Delta A. \quad (37)$$

The second term in (35) and expression (37) are close in value and they both depend on R^2. It means that the formula (34) effectively includes the contribution from adding neutrons and we can use it alone to estimate the change of nuclear polarizability between isotopes. We introduce the empirical coefficient $\zeta(A)$ to scale our prediction to the more accurately evaluated nuclear polarizabilities in Ref. [29]:

$$\zeta(A) = 0.76 + \frac{2.79}{A^{1/3}},$$

$$\alpha_p = \zeta(A)\frac{e^2 R^2 A}{40\, a_{\mathrm{sym}}}. \quad (38)$$

This final expression of nuclear polarizability is used to model the King plot nonlinearity, which grows dramatically compared to the nonlinearity found only according to the field shift formula (25), as can be seen in Table IV.

C. Many-body corrections

The results above have been obtained in the mean-field approximation. However, the isotope shifts in all waves with $|\kappa| > 1$ are dominated by the many-body effects. In the zeroth approximation, the change of the isotope changes s and $p_{1/2}$

[3]The second term with the matrix element $\langle n|x|n-1\rangle$ emerges from the single-particle consideration. In the many-body language it is the "blocking" contribution: core neutrons cannot be excited to the state occupied by the valence neutron.

electron wave functions which do not vanish at the nucleus. This produces the correction δV to the electron potential, which gives the dominating contribution to the isotope shifts of the orbitals with $|\kappa| > 1$; we will refer to this as the mean-field rearrangement effect. Therefore, in any wave the dominating term in the isotope shift is proportional to $\delta\langle r^{2\gamma_1}\rangle_{AA'}$ corresponding to $|\kappa| = 1$. However, the term with $\delta\langle r^{2\gamma_2}\rangle_{AA'}$ still appears in the transition frequencies and the logic of the section above does not change. The many-body corrections only affect the magnitude of the coefficients F_i and G_i in the isotope shift [see Eq. (19)].

Consider, for example, King plot for s-$d_{3/2}$ and s-$d_{5/2}$ transitions for Ca^+, Sr^+, Ba^+, and Yb^+ presented in Table IV. First, there are higher order terms in the expansion of the s-wave density near origin, $\sim r^{2\gamma_1+2}$. They only lead to the redefinition of the main term $\delta\langle r^{2\gamma_1}\rangle_{AA'}$ and do not produce any new physical effects. The mean-field rearrangement effect and other many-body corrections for s orbital are relatively small, $\sim$10–20%, and give contributions to the coefficient F_i which are the same for both transitions and therefore insignificant. The mean-field rearrangement effects for $d_{3/2}$ and $d_{5/2}$ are huge in comparison with the direct contributions, but their absolute values are smaller than that for $s_{1/2}$. These mean-field rearrangement effects produce some corrections to the coefficients F_i and G_i but do not give a significant contribution to the nonlinearity of the King plot. This nonlinearity comes from the direct contribution to the term $G_i\delta\langle r^{2\gamma_2}\rangle_{AA'}$ since the density of $d_{3/2}$ orbital ($\kappa = 2$) near nucleus is several orders of magnitude larger than the density of $d_{5/2}$ orbital ($\kappa = -3$). We have already taken this effect into account at the single-particle mean-field level. The IS correction to the potential δV is located at larger distances where the densities of $d_{3/2}$ and $d_{5/2}$ are approximately the same.

The nonlinear corrections may be significantly larger in atoms with several valence electrons. The density of energy levels is much higher in such systems. In this case, the second-order effects in the field shift perturbation δV in Eq. (2) may be enhanced by small energy denominators and produce large nonlinear effects in the King plot [30–34].

We want to provide a rough numerical estimate of the many-body effects to the nonlinearity of the King plot using a simple model. We have compared our mean-field approximation for s and higher waves with the accurate numerical CI+MBPT calculations used throughout [9,35,36]. Many-body correction to the s-wave field shift is not very large [35]. For the purpose of this work, we can omit this term.

However, many-body corrections for higher wave terms are found to be significant [35]. For the higher waves, δV is dominated by the corrections to the s-wave functions; therefore we model the mean-field rearrangement effect by the following expression:

$$\Delta\tilde{\varepsilon}_\kappa = \Delta\varepsilon_\kappa - \frac{\Delta\varepsilon_{s,\kappa}}{2}, \quad \Delta\varepsilon_{s,\kappa} = \Delta\varepsilon_s\left(\frac{I_\kappa}{I_s}\right)^{3/2}. \tag{39}$$

Here the initial $\Delta\varepsilon_s = \Delta E_s + \delta E_{\alpha,s}$ comprises both mean-field contribution (25) and the polarizability term (28). The ratio of ionization potentials comes from the density in the vicinity of the nucleus which is proportional to $I^{3/2}$ [see Eqs. (B2)–(B4)]. We have tested this semiempirical estimate by comparing our field shift results with accurate numerical many-body calculations [9,36]; the coefficient of 1/2 was necessary to reproduce the numerical results. It must be noted that this approximation works best for alkali-like ions such as Ca^+ and Sr^+ and is less effective in characterizing many-body effects in Yb^+ and Hg^+; in these heavier ions we expect an order of magnitude estimate of many-body effects at best.

Nonlinear corrections to the King plot may also be produced by the quadratic effects in the field shift, which we further estimate as $\pm(\Delta\varepsilon_\kappa - \frac{\Delta\varepsilon_{s,\kappa}}{2})^2/I_\kappa$.[4] Therefore, the complete formulas for the shift of an energy level will look like

$$\Delta\tilde{\tilde{\varepsilon}}_\kappa = \Delta\tilde{\varepsilon}_\kappa \pm \frac{(\Delta\tilde{\varepsilon}_\kappa)^2}{I_\kappa}. \tag{40}$$

Here I_s denotes the ionization potential of an s wave, and I_κ is that for any other wave. The quadratic effects arising from the s wave can be similarly written as

$$\Delta\tilde{\tilde{\varepsilon}}_s = \Delta\varepsilon_s \pm \frac{(\Delta\varepsilon_s)^2}{I_s}. \tag{41}$$

However, in this s-wave formula, we have omitted the many-body correction term which does not play an important role here.

King plot nonlinearity values taking into account many-body contributions are presented in Table V. As can be seen, the addition of the first-order corrections (39) does not considerably affect the nonlinearity. It should be noted that for the evaluation of many-body effects one must include all effects which have been included at the mean-field level. For example, if the field shift term (25) and the nuclear polarizability contribution (28) have been included at the mean-field level, they both must be included in the mean-field rearrangement and quadratic effects. If it contains only the first term, the resulting first- and second-order many-body effects will generate a large phantom nonlinearity in the King plot, because the dependence on the nuclear parameters (radius R and mass number A) is no longer the same for the single-electron mean-field and many-body effect.

On the other hand, the quadratic term (40) is responsible for the radical growth of the King plot nonlinearity in heavy atoms (especially for f-shell transition in Yb^+), while remaining insignificant in Ca^+ and Sr^+. Indeed, the field shift is $\propto Z^{2\gamma}$, and correspondingly the quadratic term is $\propto Z^{4\gamma}$; i.e., it very rapidly increases with the nuclear charge.

V. ESTIMATE OF THE QUADRATIC MASS SHIFT IN THE KING PLOT NONLINEARITY

For one electron above closed shells, the normal mass shift may be used as a rough estimate for the total mass shift [35,37]:

$$\Delta\varepsilon_M = -\varepsilon m_e \mu_{AA'}, \tag{42}$$

$$\Delta\tilde{\tilde{\varepsilon}}_{M2} = \pm\frac{(\Delta\varepsilon_M)^2}{I}, \tag{43}$$

[4]The quadratic effect may be enhanced if there is a close atomic level with the same angular momenta and parity which may be admixed by the IS operator. This does not happen in atoms with one electron above close shells which we consider.

TABLE V. Estimates for the nonlinearities of King plot [defined in Eq. (23)], taking into account the many-body mean-field rearrangement corrections, as shown in Eq. (39). Method 4 is based on a sum of the mean-field analytically determined contribution (25) and the first-order many-body effect ($-\Delta\varepsilon_\kappa/2$). Method 5 uses the mean-field term (25), the first-order many-body effect, and the polarizability contribution (26). The next two columns show the second-order contributions to the nonlinearity with an unknown sign arising from the quadratic terms [e.g., Eqs. (41) and (40)]. The first of them shows the quadratic corrections ignoring the nuclear polarizability α_p; i.e., it corresponds to method 4. The second of them takes into account the polarizability contribution and thus corresponds to method 5. The very last column details the nonlinearity due to the quadratic mass shift (QMS) estimated from the normal mass shift contribution as presented in Eq. (43).

							Nonlinearity (Hz)				
									Quadratic term inc. MB		
Ion	Z	A	A_1	A_2	A_3	Pair of transitions	Method 4	Method 5	Without α_p	With α_p	QMS
Ca^+	20	40	42	44	48	$3p^6 4s\ ^2S_{1/2} \to 3p^6 3d\ ^2D_{3/2}$	3.0×10^{-4}	-6.6×10^{-2}	$\pm 2.9 \times 10^{-3}$	$\pm 2.7 \times 10^{-3}$	± 3.0
						$3p^6 4s\ ^2S_{1/2} \to 3p^6 3d\ ^2D_{5/2}$					
Sr^+	38	84	86	88	90	$4p^6 5s\ ^2S_{1/2} \to 4p^6 4d\ ^2D_{3/2}$	1.1×10^{-2}	-2.6	± 0.23	± 0.25	± 9.0
						$4p^6 5s\ ^2S_{1/2} \to 4p^6 4d\ ^2D_{5/2}$					
Ba^+	56	132	134	136	138	$5p^6 6s^1\ ^2S_{1/2} \to 5p^6 5d\ ^2D_{3/2}$	-3.9×10^{-2}	7.4	∓ 2.0	∓ 1.9	∓ 1.8
						$5p^6 6s^1\ ^2S_{1/2} \to 5p^6 5d\ ^2D_{5/2}$					
Yb^+	70	168	170	172	176	$4f^{14} 6s\ ^2S_{1/2} \to 4f^{13} 6s^2\ ^2F^o_{7/2}$	-3.1	39	± 12260	± 12130	± 28
						$4f^{14} 6s\ ^2S_{1/2} \to 4f^{14} 5d\ ^2D_{3/2}$					
						$4f^{14} 6s\ ^2S_{1/2} \to 4f^{14} 5d\ ^2D_{3/2}$	3.1	-18	± 392	± 386	± 1.1
						$4f^{14} 6s\ ^2S_{1/2} \to 4f^{14} 5d\ ^2D_{5/2}$					
Hg^+	80	196	198	200	204	$5d^{10} 6s\ ^2S_{1/2} \to 5d^9 6s^2\ ^2D_{3/2}$	3.0	-13	± 2406	± 2382	± 0.38
						$5d^{10} 6s\ ^2S_{1/2} \to 5d^9 6s^2\ ^2D_{5/2}$					

where m_e is the electron mass, ε is the energy of a specific electronic level, and $\Delta\varepsilon$ is the shift in energy of this level. The nonlinearity of the King plot [see Eq. (23)] arising from the addition of the quadratic term (43) to the IS is shown in the last column of Table V. The linear normal mass shift term (42) does not contribute to the nonlinearity.

VI. NEW PARTICLE

King plot nonlinearity may result from an interaction between electrons and neutrons mediated by a new boson of mass m_ϕ [38]. The effective potential associated with such a particle would be the Yukawa potential:

$$V_\phi(r) = -q_n q_e N \frac{e^{-kr}}{r}\,,$$
$$k = \frac{m_\phi c}{\hbar}, \quad \alpha_{\rm NP} \equiv \frac{q_n q_e}{\hbar c}\,, \tag{44}$$

where N is the neutron number, q_n and q_e are particle coupling strengths to the neutrons and electrons respectively, and r is the distance from the nucleus. We aim at constraining the coupling constant $\alpha_{\rm NP}$. Let us estimate the energy shifts in atomic states that the new particle might cause. When the particle is very light ($k \ll 1/a_B$) and therefore $e^{-kr} \approx 1$, the potential (44) becomes Coulomb-like:

$$V_\phi(r) = -q_n q_e N \frac{1}{r}\,. \tag{45}$$

Making use of the virial theorem, one can express the average potential energy of the system as double total energy:

$$\langle V \rangle = 2E_{\rm tot}\,. \tag{46}$$

Substituting here values for a single outer electron in the Coulomb field $V = V_c = -(z_i+1)e^2/r$ and $E_{\rm tot} = -I_\kappa$, one obtains

$$\left\langle \frac{1}{r} \right\rangle = \frac{2I_\kappa}{(z_i+1)e^2}\,. \tag{47}$$

Therefore, the energy shift of an electron with a given κ arising from a new light particle, seen as the change of $\langle V_\phi \rangle$ between the isotopes, can be approximately written as

$$\Delta E_{\phi,\kappa} = -\frac{\alpha_{\rm NP}}{\alpha}\frac{2I_\kappa}{(z_i+1)}\Delta N. \tag{48}$$

We replaced $q_n q_e/e^2 = \alpha_{\rm NP}/\alpha$, where $\alpha = e^2/\hbar c$ is fine structure constant. For mass $m_\phi = 0$ many-body effects are not enhanced, so we do not add them.

On the other hand, the energy shifts resulting from an interaction mediated by heavier particles ($Z^{1/3}/a_B < k < 1/R$, where R is the nuclear radius and $a_B/Z^{1/3}$ is the Thomas-Fermi electron screening radius) are found by direct integration of (44) with the relativistic wave functions for a valence electron (see Appendix B):

$$\Delta E_{\phi,\kappa} = -q_n q_e \Delta N \int_0^\infty \left[f_\kappa^2(r) + g_\kappa^2(r)\right]\frac{e^{-kr}}{r} r^2 dr\,. \tag{49}$$

For larger masses, $Z/a_B < k < 1/R$, it is instructive to present also the approximate formula for (49) which shows dependence on the Compton wavelength $k = \frac{m_\phi c}{\hbar}$ and other parameters explicitly:

$$\Delta E_{\phi,\kappa} = -\frac{\alpha_{\rm NP}}{\alpha}\frac{4\kappa(\kappa-\gamma)}{(z_i+1)Z}\frac{\Gamma(2\gamma)}{[\Gamma(2\gamma+1)]^2}\left(\frac{2Z}{ka_B}\right)^{2\gamma}$$
$$\times \frac{I_\kappa^{3/2}}{{\rm Ry}^{1/2}}\Delta N\,. \tag{50}$$

The effect of very heavy bosons with $k > 1/R$ is absorbed into the usual field shift (proportional to $R^{2\gamma}$), as the range of the interaction is less than the nuclear radius. It is therefore nearly impossible to see this new physics effect against the background of nuclear uncertainties. We restrict

TABLE VI. Values of the ratio $\frac{\alpha_{NP}}{\alpha}$ of the coupling constant α_{NP} for a new boson with mass m_ϕ to the fine structure constant α. They correspond to the most significant King plot nonlinearity value that can arise from SM corrections to the IS (see Table V). Individual isotope shifts consist of the s-wave contribution, which does not give rise to any nonlinearity, and the new particle contributions (48) and (49) for light ($m_\phi \to 0$) and heavier particles respectively.

Ion	Z	A	A_1	A_2	A_3	Pair of transitions	Nonlinearity (Hz)	$\frac{\alpha_{NP}}{\alpha}$ $m_\phi \to 0$	$m_\phi = 10^5$ eV	$m_\phi = 10^6$ eV	$m_\phi = 10^7$ eV
Ca^+	20	40	42	44	48	$3p^6 4s\ ^2S_{1/2} \to 3p^6 3d\ ^2D_{3/2}$	−3.0	5.6×10^{-12}	1.4×10^{-9}	-9.9×10^{-9}	-7.2×10^{-7}
						$3p^6 4s\ ^2S_{1/2} \to 3p^6 3d\ ^2D_{5/2}$					
Sr^+	38	84	86	88	90	$4p^6 5s\ ^2S_{1/2} \to 4p^6 4d\ ^2D_{3/2}$	−11.9	6.7×10^{-13}	5.5×10^{-11}	-7.4×10^{-10}	-3.8×10^{-8}
						$4p^6 5s\ ^2S_{1/2} \to 4p^6 4d\ ^2D_{5/2}$					
Ba^+	56	132	134	136	138	$5p^6 6s^1\ ^2S_{1/2} \to 5p^6 5d\ ^2D_{3/2}$	11.1	7.7×10^{-13}	3.9×10^{-11}	-3.4×10^{-8}	-3.3×10^{-7}
						$5p^6 6s^1\ ^2S_{1/2} \to 5p^6 5d\ ^2D_{5/2}$					
Yb^+	70	168	170	172	176	$4f^{14} 6s\ ^2S_{1/2} \to 4f^{13} 6s^2\ ^2F^o_{7/2}$	12190	-2.5×10^{-11}	2.4×10^{-9}	1.3×10^{-8}	3.2×10^{-7}
						$4f^{14} 6s\ ^2S_{1/2} \to 4f^{14} 5d\ ^2D_{3/2}$					
						$4f^{14} 6s\ ^2S_{1/2} \to 4f^{14} 5d\ ^2D_{3/2}$	−406	2.7×10^{-11}	2.2×10^{-9}	-1.7×10^{-8}	-3.9×10^{-7}
						$4f^{14} 6s\ ^2S_{1/2} \to 4f^{14} 5d\ ^2D_{5/2}$					
Hg^+	80	196	198	200	204	$5d^{10} 6s\ ^2S_{1/2} \to 5d^9 6s^2\ ^2D_{3/2}$	−2395	-1.8×10^{-10}	6.6×10^{-8}	-5.5×10^{-8}	-1.0×10^{-6}
						$5d^{10} 6s\ ^2S_{1/2} \to 5d^9 6s^2\ ^2D_{5/2}$					

our consideration with masses corresponding to $k < 1/R$, i.e., $m_\phi \lesssim 30$ MeV.

We also take into account the characteristic value of many-body mean-field rearrangement corrections. We estimate these many-body effects in a similar manner to the corrections to the isotope shift seen in (39). The mean-field rearrangement effect can be modeled as

$$\Delta\tilde{E}_{\phi,\kappa} = \Delta E_{\phi,\kappa} - \frac{\Delta E_{\phi,s,\kappa}}{2}, \quad \Delta E_{\phi,s,\kappa} = \Delta E_{\phi,s}\left(\frac{I_\kappa}{I_s}\right)^{3/2}. \tag{51}$$

The coefficient $1/2$ arises from comparisons of the electronic part of the integral (49) (omitting ΔN) with accurate numerical many-body calculations of the same quantity performed in Ref. [9]. Many-body effects are taken into account for higher waves only.

As always, the IS of a transition frequency would be the difference of the shifts of two levels $\Delta E_{\phi,\kappa}$. We examine the nonlinearity arising from the addition of these terms to otherwise linear King plot. First, we construct the linear King plot leaving only the mean field s-wave contribution of the form (25) in all transitions and then we add the new particle contribution to this linear King plot. Then we examine the sensitivity of nonlinearity to the coupling constant $\frac{\alpha_{NP}}{\alpha}$ by equating the nonlinearity which appears as a result of including a new particle and the nonlinearity emerging naturally from SM. The values of $\frac{\alpha_{NP}}{\alpha}$ that lead to the same nonlinearity as SM corrections in a given pair of transitions are presented in Table VI.

VII. CONCLUSIONS

The analytical formula for the field isotope shift (11) gives reasonable accuracy of the estimates for the transitions involving s-wave electron. In superheavy elements, it should also describe the $p_{1/2}$-wave field IS which is comparable to the s-wave shift. For higher waves, the field IS is dominated by the many-body corrections which are in turn dominated by the mean-field rearrangement effect. The latter is produced by the IS of the mean field potential due to IS of the s-electron wave functions.

In the single-particle mean-field approximation, the nonlinearity of the King plot is strongly dominated by the nuclear polarizability contribution (see Table IV). However, the quadratic field shift, which very rapidly increases with the nuclear charge Z and gives the dominating contribution to the nonlinearity of the King plot in heavy atoms, is not so sensitive to the nuclear polarizability contribution (see Table V). However, in medium atoms the quadratic terms are not so large; therefore, the measurements of the nonlinearity of the King plot may, in principle, be used to extract the nuclear polarizability differences between the isotopes.

The contribution of the hypothetical new light boson increases with the nuclear charge Z. However, the quadratic contribution to the field IS increases with Z much faster. In light atoms, the nonlinearity is dominated by the quadratic mass shift. Therefore, it may be easier to extract a competitive limit on the new particle interaction strength from the measured nonlinearity of the King plot in medium atom transitions such as s-d transitions in Sr^+ and Yb^+; see Table VI.

The field IS may be an order of magnitude smaller in transitions which do not involve s-wave electrons. This means that the dominating source of the King plot nonlinearity in heavy atoms, the quadratic field IS term, may be much smaller. Such transitions may, in principle, provide better accuracy for the new low-mass particle. However, these must be transitions with a small natural width. In all existing optical atomic clocks such narrow transitions always involve an s electron. Therefore, to explore such possibility, we should look for narrow transitions in atoms and ions containing p, d, or f electrons in the ground open shell or low-energy excitations from the closed f, d, p shells.

ACKNOWLEDGMENTS

This work was supported by the Australian Research Council and the Gutenberg Research College. The authors are grateful to S. Karshenboim, D. Budker, K. Pachucki, M. Pospelov, V. Shabaev, and E. Fuchs for valuable discussions and corrections. A.V.V. would like to thank UNSW, Australia, for hospitality.

APPENDIX A: RELATIVISTIC ELECTRON WAVE FUNCTION INSIDE NUCLEUS

The s and $p_{1/2}$ approximate wave functions within the nucleus in a neutral atom are presented in Refs. [16,39]. We have introduced minor changes to extend the result to ions with charge z_i. Denoting $x = r/R$, the upper and lower radial components of the s wave function can be given:

$$f_s = A_s\left[1 - \frac{3}{8}Z^2\alpha^2x^2\left(1 - \frac{4}{15}x^2\right)\right], \tag{A1}$$

$$g_s = -\frac{1}{2}A_sZ\alpha x \times\left[1 - \frac{1}{5}x^2 - \frac{9}{40}Z^2\alpha^2x^2\left(1 - \frac{3}{7}x^2 + \frac{4}{81}x^4\right)\right], \tag{A2}$$

where A_s is a constant defined as

$$A_s = \frac{2}{(z_i+1)^{1/2}}\frac{2\left(\frac{a_B}{2ZR}\right)^{1-\gamma}}{\Gamma(2\gamma+1)}\left(\frac{Z}{a_B^3}\right)^{1/2} \times\left(\frac{I}{\mathrm{Ry}}\right)^{3/4}\left(1 - \frac{1}{40}Z^2\alpha^2\right). \tag{A3}$$

Here $\gamma = \sqrt{\kappa^2 - Z^2\alpha^2}$, and $I = \frac{(z_i+1)^2}{\nu^2}\mathrm{Ry}$ is the ionization energy with effective principal quantum number ν and $\mathrm{Ry} = \frac{e^2}{2a_B}$.

The radial $p_{1/2}$ wave functions are written in terms of the radial s wave functions in the following way:

$$f_p = -\frac{A_p}{A_s}\,g_s\,, \tag{A4}$$

$$g_p = i\frac{A_p}{A_s}\,f_s\,. \tag{A5}$$

Here A_p is

$$A_p = \frac{Z\alpha}{(z_i+1)^{1/2}}\frac{2\left(\frac{a}{2ZR}\right)^{1-\gamma}}{\Gamma(2\gamma+1)}\left(\frac{Z}{a_B^3}\right)^{1/2} \times\left(\frac{I}{\mathrm{Ry}}\right)^{3/4}\left(1 + \frac{9}{40}Z^2\alpha^2\right). \tag{A6}$$

APPENDIX B: RELATIVISTIC WAVE FUNCTION FOR A VALENCE ELECTRON AT $r \ll a_B/Z^{1/3}$

At short distances $r \ll a_B/Z^{1/3}$, the nuclear Coulomb potential is not screened and the valence electron energy may be neglected. The solution of the Dirac equation can be expressed in terms of Bessel functions; see, e.g., Ref. [16].

$$f_\kappa = \frac{C}{r}\left[(\gamma+\kappa)J_{2\gamma}(y) - \frac{y}{2}J_{2\gamma-1}(y)\right], \tag{B1}$$

$$g_\kappa = \frac{C}{r}(Z\alpha)J_{2\gamma}(y), \tag{B2}$$

$$y = \sqrt{\frac{8Zr}{a_B}}, \tag{B3}$$

$$C = \frac{\kappa}{|\kappa|}\frac{1}{\sqrt{Za_B(z_i+1)}}\left(\frac{I}{\mathrm{Ry}}\right)^{3/4}. \tag{B4}$$

Again, we introduced factor $(z_i + 1)$ to account for ion wave functions.

APPENDIX C: RELATIVISTIC WAVE FUNCTION FOR A VALENCE ELECTRON AT $r \ll a_B/Z$

The Bessel functions have power asymptotic at $r \ll a_B/Z$. From power expansions of (B1) and (B2), one obtains the following expression for the electron wave functions outside the nucleus [14,16]:

$$f_\kappa(r) = \frac{1}{(z_i+1)^{1/2}}\frac{\kappa}{|\kappa|}(\kappa-\gamma)\left(\frac{Z}{a_B^3}\right)^{1/2} \times\left(\frac{I}{\mathrm{Ry}}\right)^{3/4}\frac{2}{\Gamma(2\gamma+1)}\left(\frac{a_B}{2Zr}\right)^{1-\gamma}, \tag{C1}$$

$$g_\kappa(r) = \frac{1}{(z_i+1)^{1/2}}\frac{\kappa}{|\kappa|}Z\alpha\left(\frac{Z}{a_B^3}\right)^{1/2} \times\left(\frac{I}{\mathrm{Ry}}\right)^{3/4}\frac{2}{\Gamma(2\gamma+1)}\left(\frac{a_B}{2Zr}\right)^{1-\gamma}. \tag{C2}$$

APPENDIX D: IONIZATION POTENTIALS FOR ISOTOPE SHIFT AND KING PLOT CALCULATIONS

The ionization potentials of the $7s$ electrons for the superheavy elements $Z = 98$–102 are taken from the NIST database [40]. Those include experimental values 50 665 and 51 358 cm^{-1} for $Z = 98,99$, semiempirical evaluations 52 400 and 53 100 cm^{-1} ($Z = 100,101$), and a theoretical calculation 53 740 cm^{-1} ($Z = 102$). The ionization potential 59 462 cm^{-1} of Rf ($Z = 104$) is roughly estimated as the average of potentials for $Z = 102$ and $Z = 105$ due to the lack of reliable information.

The energies for $7p$ electrons in $Z = 98,99,102$ are derived from the experimental values of the relevant transitions 27 779, 19 788, and 29 961 cm^{-1} [41,42] and in ($Z = 104$) the energy of the transition 20 347 cm^{-1} is based on a numerical prediction [43]. For Fm ($Z = 100$) and Md ($Z = 101$), the $7p$ ionization potential is taken to be the average of known Es ($Z = 99$) and No ($Z = 102$) potentials, 27 675 cm^{-1}.

For elements $Z = 105$–112, we use numerical values of $7s$ and $7p$ ionization potentials [44].

Furthermore, the p ground-state ionization energy in Lr is measured to be 40 005 cm^{-1} [45]. The upper s state was found by subtracting the $p \to s$ calculated transition frequency of 20 253 cm^{-1} [43] to give an ionization potential of 19 800 cm^{-1}. Recent atomic structure calculations were used to find the potentials for the ground p states and excited s states for Nh and Fl. For the Nh p state, we used 59 770 cm^{-1} and the s state ionization potential of 23 729 cm^{-1} [46]. Similarly, for the Fl p state we used 68 868 cm^{-1} [47], a $p \to s$ transition energy of 43 876 cm^{-1} [46] to give an s-state ionization potential of 24 992 cm^{-1}.

Ionization potentials and transition energies for King plot nonlinearity estimates were taken from the NIST database [40].

[1] Y. T. Oganessian, V. K. Utyonkov, Y. V. Lobanov, F. S. Abdullin, A. N. Polyakov, I. V. Shirokovsky, Y. S. Tsyganov, G. G. Gulbekian, S. L. Bogomolov, B. N. Gikal *et al.*, Nucl. Phys. A **734**, 109 (2004).

[2] J. H. Hamilton, S. Hofmann, and Y. T. Oganessian, Annu. Rev. Nucl. Part. Sci. **63**, 383 (2013).

[3] G. M. Fuller, A. Kusenko, and V. Takhistov, Phys. Rev. Lett. **119**, 061101 (2017).

[4] S. Goriely, A. Bauswein, and H.-T. Janka, Astrophys. J. Lett. **738**, L32 (2011).

[5] A. Frebel and T. C. Beers, Phys. Today **71**, 30 (2018).

[6] V. F. Gopka, A. V. Yushchenko, V. A. Yushchenko, I. V. Panov, and C. Kim, Kinematics Phys. Celestial Bodies **24**, 89 (2008).

[7] V. A. Dzuba, V. V. Flambaum, and J. K. Webb, Phys. Rev. A **95**, 062515 (2017).

[8] E. Witten, Phys. Rev. D **30**, 272 (1984).

[9] J. C. Berengut, D. Budker, C. Delaunay, V. V. Flambaum, C. Frugiuele, E. Fuchs, C. Grojean, R. Harnik, R. Ozeri, G. Perez *et al.*, Phys. Rev. Lett. **120**, 091801 (2018).

[10] G. Racah, Nature (London) **129**, 723 (1932).

[11] J. E. Rosenthal and G. Breit, Phys. Rev. **41**, 459 (1932).

[12] W. H. King, *Isotope Shifts in Atomic Spectra* (Springer Science & Business Media, Berlin, 2013).

[13] V. M. Shabaev, J. Phys. B: At. Mol. Opt. Phys. **26**, 1103 (1993).

[14] I. I. Sobelman, *Introduction to the Theory of Atomic Spectra* (Pergamon, Oxford, 1972).

[15] A. Papoulia, B. G. Carlsson, and J. Ekman, Phys. Rev. A **94**, 042502 (2016).

[16] I. B. Khriplovich, *Parity Nonconservation in Atomic Phenomena*, 2nd ed. (Gordon and Breach, Philadelphia, 1991).

[17] F. Gebert, Y. Wan, F. Wolf, C. N. Angstmann, J. C. Berengut, and P. O. Schmidt, Phys. Rev. Lett. **115**, 053003 (2015).

[18] G. Fricke and K. Heilig, *Nuclear Charge Radii*, Elementary Particles, Nuclei, and Atoms Vol. 20 (Springer-Verlag, Berlin, 2004).

[19] R. F. G. Ruiz, M. L. Bissell, K. Blaum, A. Ekström, N. Frömmgen, G. Hagen, M. Hammen, K. Hebeler, J. D. Holt, G. R. Jansen *et al.*, Nat. Phys. **12**, 594 (2016).

[20] W. H. King, JOSA **53**, 638 (1963).

[21] M. Puchalski and K. Pachucki, Hyperfine Interact. **196**, 35 (2010).

[22] V. A. Dzuba, V. V. Flambaum, P. G. Silvestrov, and O. P. Sushkov, J. Phys. B: At. Mol. Phys. **20**, 1399 (1987).

[23] K. Pachucki, M. Weitz, and T. W. Hänsch, Phys. Rev. A **49**, 2255 (1994).

[24] A. B. Migdal, J. Exp. Theor. Phys. **15**, 81 (1945).

[25] J. S. Levinger, Phys. Rev. **107**, 554 (1957).

[26] C. F. von Weizsäcker, Z. Phys. **96**, 431 (1935).

[27] A. E. S. Green, Phys. Rev. **95**, 1006 (1954).

[28] L. D. Landau and E. M. Lifshitz, *Quantum Mechanics: Non-relativistic Theory* (Pergamon, London, 1958).

[29] J. Piekarewicz, B. K. Agrawal, G. Colò, W. Nazarewicz, N. Paar, P.-G. Reinhard, X. Roca-Maza, and D. Vretenar, Phys. Rev. C **85**, 041302(R) (2012).

[30] J. A. R. Griffith, G. R. Isaak, R. New, and M. P. Ralls, J. Phys. B: At. Mol. Phys. **14**, 2769 (1981).

[31] C. W. P. Palmer and D. N. Stacey, J. Phys. B: At. Mol. Phys. **15**, 997 (1982).

[32] E. C. Seltzer, Phys. Rev. **188**, 1916 (1969).

[33] S. A. Blundell, P. E. G. Baird, C. W. P. Palmer, D. N. Stacey, and G. K. Woodgate, J. Phys. B: At. Mol. Phys. **20**, 3663 (1987).

[34] G. Torbohm, B. Fricke, and A. Rosén, Phys. Rev. A **31**, 2038 (1985).

[35] J. C. Berengut, V. A. Dzuba, and V. V. Flambaum, Phys. Rev. A **68**, 022502 (2003).

[36] J. C. Berengut (private communication).

[37] M. S. Safronova and W. R. Johnson, Phys. Rev. A **64**, 052501 (2001).

[38] C. Delaunay, R. Ozeri, G. Perez, and Y. Soreq, Phys. Rev. D **96**, 093001 (2017).

[39] V. V. Flambaum and J. S. M. Ginges, Phys. Rev. A **65**, 032113 (2002).

[40] A. Kramida, Y. Ralchenko, J. Reader, and NIST ASD Team, *NIST Atomic Spectra Database (ver. 5.3)* (National Institute of Standards and Technology, Gaithersburg, MD, 2017).

[41] J. E. Sansonetti and W. C. Martin, J. Phys. Chem. Ref. Data **34**, 1559 (2005).

[42] M. Laatiaoui, W. Lauth, H. Backe, M. Block, D. Ackermann, B. Cheal, P. Chhetri, C. E. Düllmann, P. van Duppen, J. Even *et al.*, Nature (London) **538**, 495 (2016).

[43] V. A. Dzuba, M. S. Safronova, and U. I. Safronova, Phys. Rev. A **90**, 012504 (2014).

[44] V. A. Dzuba (private communication).

[45] T. K. Sato, M. Asai, A. Borschevsky, T. Stora, N. Sato, Y. Kaneya, K. Tsukada, C. E. Düllmann, K. Eberhardt, E. Eliav, *et al.*, Nature (London) **520**, 209 (2015).

[46] T. H. Dinh and V. A. Dzuba, Phys. Rev. A **94**, 052501 (2016).

[47] A. Landau, E. Eliav, Y. Ishikawa, and U. Kaldor, J. Chem. Phys. **114**, 2977 (2001).